Spectral analysis of block structured nonlinear systems

Preprints of the 18th IFAC World Congress
Milano (Italy) August 28 - September 2, 2011

Spectral Analysis of Block Structured Nonlinear Systems ⋆

David Rijlaarsdam [*,**] **Pieter Nuij** [*] **Johan Schoukens** [**] **Maarten Steinbuch** [*]

[*] *Eindhoven University of Technology*
Department of Mechanical Engineering, Control Systems Technology
PO Box 513, WH -1.133, 5600 MB, Eindhoven, The Netherlands
[**] *Vrije Universiteit Brussel*
Department of Fundamental Electricity and Instrumentation
K430, Pleinlaan 2, 1050 Brussels, Belgium

Abstract: It is a challenge to investigate if frequency domain methods can be used for the analysis or even synthesis of nonlinear dynamical systems. However, the effects of nonlinearities in the frequency domain are non-trivial. In this paper analytical tools and results to analyze nonlinear systems in the frequency domain are presented. First, an analytical relationship between the parameters defining the nonlinearity, the LTI dynamics and the output spectrum is derived. These results allow analytic derivation of the corresponding higher order sinusoidal input describing functions (HOSIDF). This in turn allows to develop novel identification algorithms for the HOSIDFs using identification experiments that apply broadband excitation signals, which significantly reduces the experimental burden previously associated with obtaining the HOSIDFs. Finally, two numerical examples are presented. These examples illustrate the use and efficiency of the theoretical results in the analysis of the effects of nonlinearities in the frequency domain and broadband identification of the HOSIDFs.

Keywords: nonlinear systems, spectral analysis, frequency response methods, describing functions, identification algorithms, system identification

1. INTRODUCTION

The frequency response function (FRF) is frequently used to model dynamical systems in the frequency domain. In the presence of nonlinearities, however, this type of frequency domain model fails to model the complete dynamics, which may lead to unexpected and undesired results. In order to use frequency domain data to analyze nonlinear systems, the effects of nonlinearities in the frequency domain need to be taken into account.

The effects of nonlinearities in the frequency domain have been analyzed in literature in various ways. First, in Billings and Tsang (1989), the authors use a generalized FRF, related to the Volterra kernel, to describe nonlinear systems in the frequency domain. This work is continued over the years and recent results are published in Jing et al. (2009); Li and Billings (2010). Second, a different approach is used in Pavlov et al. (2007a). Here, a FRF for nonlinear systems is introduced that fully models the input-output behavior of uniformly convergent nonlinear systems subject to harmonic inputs. Moreover, a nonlinear bodeplot is defined and extended to closed loop nonlinear systems in Pavlov et al. (2007b) by defining a nonlinear (complementary) sensitivity function. Third, in Pintelon and Schoukens (2001), an extensive discussion of frequency domain identification methods is provided. The authors use specially designed multisine excitation signals to obtain quantitative measures for the level and type of nonlinearities present. Recent results concerning the robustness of the obtained models are presented in Schoukens et al. (2009). Fourth, in Nuij et al. (2006) the Higher Order Sinusoidal Input Describing Functions (HOSIDFs) are defined. The HOSIDFs are an extension of the sinusoidal input describing function and describe the response (gain and phase) at harmonics of the base frequency of a sinusoidal input signal. Identification of the HOSIDFs in a closed loop setting is discussed in Nuij et al. (2008a) while HOSIDFs are used to identify friction parameters in Nuij et al. (2008b). In Rijlaarsdam et al. (2010a,c,d) the HOSIDFs are compared to the FRF and used to tune nonlinear controllers. Finally, in Rijlaarsdam et al. (2010b) analytical expressions for the HOSIDFs are derived for a class of nonlinear systems. This allows for frequency domain analysis of the effects of the parameters defining the nonlinear and LTI dynamics and identification of the HOSIDFs using broadband excitation signals.

In this paper, part of the results in Rijlaarsdam et al. (2010b) are used and applied to analyze and identify nonlinear systems in the frequency domain. In Section 3

⋆ This work is carried out as part of the Condor project, a project under the supervision of the Embedded Systems Institute (ESI) and with FEI company as the industrial partner. This project is partially supported by the Dutch Ministry of Economic Affairs under the BSIK program. This work was supported in part by the Fund for Scientific Research (FWO-Vlaanderen), by the Flemish Government (Methusalem), and by the Belgian Government through the Interuniversity Poles of Attraction (IAP VI/4) Program. Corresponding author D.J. Rijlaarsdam, david@davidrijlaarsdam.nl, Tel. +31645410004, Fax +31402461418.

an analysis of the effects of nonlinearities on the output spectrum of a class of nonlinear systems is provided. Furthermore, the corresponding HOSIDFs are analyzed. In Section 4, two numerical examples are provided. The first example illustrates the use of the theoretical results to the spectral analysis of nonlinear systems. Finally, the second example applies the theoretical results in an identification setting to measure the HOSIDFs using broadband excitation signals. Matlab tools to apply the theory presented in this paper are available online [1].

2. NOMENCLATURE

In the following analysis, continuous spectra and vectors containing only specific spectral components are used. Time signals $x(t) \in \mathbb{R}$ are denoted by non-capitalized roman letters, while the corresponding single sided spectra $\mathscr{X}(\omega) \in \mathbb{C}$ are denoted in capitalized, calligraphic font. Next, $X \in \mathbb{C}$, denoted in capitalized roman letters, denotes a vector such that $X[\ell] = \mathscr{X}\big((\ell-1)\omega_0\big)$. Hence, the ℓ^{th} element of the vector X, $X[\ell]$, contains the spectral components $\mathscr{X}(k\omega_0)$, $k = 0, 1, 2, 3, \ldots$ at the $k = (\ell-1)^{\text{th}}$ harmonic of the excitation frequency $\omega_0 \in \mathbb{R}_{>0}$. Finally, the results presented in this paper concern a class of $\overline{\mathbb{LPL}}$ nonlinear systems, which is defined below.

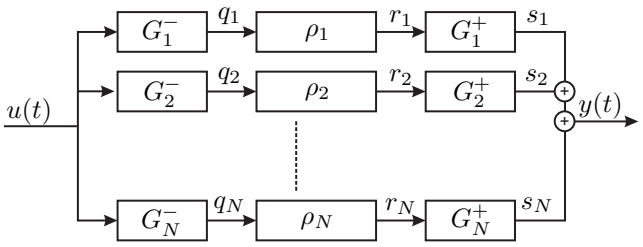

Fig. 1. $\overline{\mathbb{LPL}}$ block structured system.

Definition 1. ($\overline{\mathbb{LPL}}$: block structures).
Consider a N-branch, block structured configuration as depicted in Figure 1. Each branch consists of a series connection of a LTI block $G_n^-(\omega)$, a static nonlinear mapping ρ_n and another LTI block $G_n^+(\omega)$. The system has one input $u(t)$, one output $y(t)$ and intermediate signals $q_n(t)$, $r_n(t)$ and $s_n(t)$. The nonlinearity $\rho_n : \mathbb{R} \mapsto \mathbb{R}$ is a static, polynomial mapping of degree P_n:

$$\rho_n : r_n(t) = \sum_{p=1}^{P_n} \alpha_p^{[n]} q_n^p(t) \tag{1}$$

with $\alpha_p^{[n]} \in \mathbb{R}$. Finally, note that if $G_n^-(\omega) = 1 \; \forall \; \omega \in \mathbb{R}, n \in \mathbb{N}_1$ the remaining $\overline{\mathbb{PL}}$ system equals a parallel Hammerstein configuration with polynomial nonlinearities.

3. SPECTRAL ANALYSIS OF NONLINEAR SYSTEMS

3.1 Output Spectra of $\overline{\mathbb{LPL}}$ Systems

A detailed analysis of the spectral properties of nonlinear systems is provided in Rijlaarsdam et al. (2010b). Relevant results in this reference are reviewed briefly in this section. After analyzing the effects of a static polynomial nonlinearity in the frequency domain, results are generalized to the spectral analysis of $\overline{\mathbb{LPL}}$ systems. Finally, the analytical expressions for the output spectra of $\overline{\mathbb{LPL}}$ systems are used to analytically describe the corresponding (Fundamental) Higher Order Sinusoidal Input Describing Functions.

Consider the following static polynomial mapping:

$$y(t) = \sum_{p=1}^{P} \alpha_p u^p(t), \tag{2}$$

with $u(t),\ y(t) \in \mathbb{R}$ the input and output of the system and $\alpha_p \in \mathbb{R}$ the polynomial coefficients. Next, consider the analysis of the output spectrum $\mathscr{Y}(\omega)$ when system (2) is subject to a one-tone input:

$$u(t) = \gamma \cos(\omega_0 t + \varphi_0), \tag{3}$$

with $\gamma,\ \varphi_0 \in \mathbb{R}$ the gain and phase and $\omega_0 \in \mathbb{R}_{>0}$ the frequency of the input signal.

The output spectrum $\mathscr{Y}(\omega)$ of (2) subject to (3) depends only on the polynomial coefficients α_p and the properties of the input signal which is formalized in Theorem 1.

Theorem 1. (nonlinear coef. and output spectra).
Consider a static polynomial mapping (2), subject to an input (3). Then the single sided spectrum of the output $y(t)$ is given by the following mapping $\mathbb{R}^P \mapsto \mathbb{C}^{P+1}$, from the polynomial coefficients $\boldsymbol{\alpha}$ to the output spectrum $\mathscr{Y}(\omega)$:

$$Y = \Phi(\varphi_0)\, \Omega\, \Gamma(\gamma)\boldsymbol{\alpha}, \tag{4}$$

where the different components are defined below.

- *output spectrum (vector)* $Y \in \mathbb{C}^{P+1}$: where $Y = [\mathscr{Y}(0) \;\; \mathscr{Y}(\omega_0) \;\; \mathscr{Y}(2\omega_0) \;\; \ldots \;\; \mathscr{Y}(P\,\omega_0)]^T$ is a vector containing the nonzero spectral lines in the output spectrum, at harmonics of the input frequency.
- *input phase matrix* $\Phi(\varphi_0) \in \mathbb{C}^{(P+1)\times(P+1)}$: describing the influence of the input phase on the output spectrum: $\Phi_{k+1,k+1}(\varphi_0) = e^{ik\varphi_0},\ k = 0, 1, 2, \ldots$ and 0 otherwise.
- *input gain matrix* $\Gamma(\gamma) \in \mathbb{R}^{P\times P}$: describing the influence of the input amplitude on the output spectrum: $\Gamma_{p,p}(\gamma) = \left(\frac{\gamma}{2}\right)^p$ and 0 otherwise.
- *inter-harmonic gain matrix* $\Omega \in \mathbb{R}^{(P+1)\times P}$: describing the relation between the input and the harmonic components in the output spectrum:

$$\Omega_{1p} = \; (1-\sigma_p)\binom{p}{\frac{p}{2}}\frac{p}{2}$$

$$\Omega_{(k+1)p} = \qquad 2\binom{p}{\frac{p-k}{2}}\sigma_{pk} \quad \forall\, k \le p, k \in \mathbb{N}_1$$

  and 0 otherwise. With $\sigma_p = p \mod 2$, $\sigma_k = k \mod 2$ and $\sigma_{pk} = \sigma_p\sigma_k + (1-\sigma_p)(1-\sigma_k)$.
- *polynomial coefficients* $\boldsymbol{\alpha} \in \mathbb{R}^P$:
  where $\boldsymbol{\alpha} = [\alpha_1 \; \alpha_2 \; \ldots \; \alpha_p]^T$ is a vector containing the coefficients of the polynomial nonlinearity.

(Proof: Rijlaarsdam et al. (2010b))

Theorem 1 allows to express the output spectra of $\overline{\mathbb{LPL}}$ systems in terms of the polynomial coefficients $\boldsymbol{\alpha}^{[n]}$ and the LTI dynamics $G_n^{\pm}(\omega)$ (Matlab tool available [1]). These

[1] www.davidrijlaarsdam.nl

expressions are formulated in terms of the input gain and phase matrices $\Gamma(\gamma), \Phi(\varphi_0)$ and the inter-harmonic gain matrix Ω and yield expressions for the higher order sinusoidal input describing functions of $\overline{\mathbb{LPL}}$ systems.

3.2 Higher Order Sinusoidal Input Describing Functions

In Nuij et al. (2006), the output of a uniformly convergent, time invariant nonlinear system (Pavlov et al. (2004)), subject to (3) is considered. This output is composed of harmonics of the input frequency and equals:

$$y(t) = \sum_{k=0}^{K} |\mathfrak{H}_k(\omega_0, \gamma)|\gamma^k \cos\big(k(\omega_0 t + \varphi_0) + \angle\mathfrak{H}_k(\omega_0, \gamma)\big),$$

where $\mathfrak{H}_k(\omega_0, \gamma) \in \mathbb{C}$ is the k^{th} order Higher Order Sinusoidal Input Describing Function (HOSIDF), describing the response (gain and phase) at harmonics of the base frequency of a sinusoidal input signal.

Definition 2. ($\mathfrak{H}_k(\omega, \gamma)$: HOSIDF).
Consider a uniformly convergent, time invariant nonlinear system (Pavlov et al. (2004)) subject to (3). Define the systems output $y(t)$ and corresponding single sided spectra of the input and output $\mathscr{U}(\omega)$, $\mathscr{Y}(\omega) \in \mathbb{C}$. Then, the k^{th} higher order sinusoidal input describing function $\mathfrak{H}_k(\omega_0, \gamma) \in \mathbb{C},\ k = 0, 1, 2, \ldots$ is defined as:

$$\mathfrak{H}_k(\omega_0, \gamma) = \frac{\mathscr{Y}(k\omega_0)}{\mathscr{U}^k(\omega_0)}, \tag{5}$$

(adopted from Rijlaarsdam et al. (2010b))

Theorem 1 yields analytic expressions for the output spectra and hence the HOSIDFs of $\overline{\mathbb{LPL}}$ systems.

Lemma 1. (HOSIDFs of $\overline{\mathbb{LPL}}$ systems).
The HOSIDFs of a $\overline{\mathbb{LPL}}$ system are given by:

$$H(\omega_0, \gamma, G_n^{\pm}) = \tag{6}$$
$$\Upsilon^{-1} \sum_{n=1}^{N} \Delta(\omega_0)\, G_n^{+}(\omega) \Big[\Phi(\angle G_n^{-}(\omega_0))\Omega\Gamma(|G_n^{-}(\omega_0)|\gamma)\boldsymbol{\alpha}^{[n]}\Big],$$

with $\Delta(\omega_0) = \mathrm{diag}([\delta(\omega - 0)\ \delta(\omega - \omega_0)\ \delta(\omega - 2\omega_0)\ \ldots\ \delta(\omega - P_n\omega_0)]) \in \mathbb{R}^{(P_n+1)\times(P_n+1)}$ is a diagonal matrix of δ-functions, $H = [\mathfrak{H}_0(\omega_0)\ \mathfrak{H}_1(\omega_0)\ \mathfrak{H}_2(\omega_0)\ \ldots\ \mathfrak{H}_{\max_n P_n}(\omega_0)]^T$ and the gain compensation matrix $\Upsilon_{k+1,k+1}(\gamma) = \gamma^k$ and 0 otherwise. (Proof: Rijlaarsdam et al. (2010b))

Finally, for $\overline{\mathbb{PL}}$ systems, Lemma 1 yields the following, amplitude independent basis functions for the HOSIDFs.

Definition 3. (fHOSIDFs of $\overline{\mathbb{PL}}$ systems).
The Fundamental Higher Order Sinusoidal Input Describing functions (fHOSIDF) $\mathfrak{F}_p(\omega)$ of a $\overline{\mathbb{PL}}$ system equal a weighted sum of the LTI dynamics $G_n^{+}(\omega)$ when the system is re-formulated with respect to the set of polynomial mappings $\rho_n : r_n(t) = q_n^n$. Hence,

$$\mathfrak{F}_p(\omega) = \sum_{n=1}^{N} G_n^{+}(\omega)\alpha_p^{[n]} \tag{7}$$

The fHOSIDFs are amplitude independent basis functions for the HOSIDFs which provide a decoupling of the amplitude and frequency effects in the HOSIDFs, since:

$$H(\omega_0, \gamma, G_n^{+}) = \big[\Upsilon^{-1}(\gamma)\Delta(\omega_0)\,\Omega\,\Gamma(\gamma)\big]\, F(\omega),$$

with $F(\omega) = [\mathfrak{F}_1(\omega)\ \mathfrak{F}_2(\omega)\ \ldots\ \mathfrak{F}_{\max_n P_n}(\omega)]^T$. (Proof: Rijlaarsdam et al. (2010b))

Next, these theoretical results are applied (Matlab tool available [1]) to analyze and identify two nonlinear systems in the frequency domain.

4. NUMERICAL RESULTS

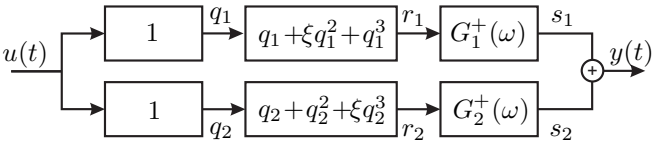

Fig. 2. Two-branch $\overline{\mathbb{PL}}$ system.

Consider the $\overline{\mathbb{PL}}$ system depicted in Figure 2, which is a $\overline{\mathbb{LPL}}$ system with $N = 2$, $\boldsymbol{\alpha}^{[1]} = [1\ \xi\ 1]^T$, $\boldsymbol{\alpha}^{[2]} = [1\ 1\ \xi]^T$ and $G_n^{-}(\omega) = 1$. Definition 3 yields analytic expressions for the fHOSIDFs of the system depicted in Figure 2:

$$F(\omega) = \begin{bmatrix} \mathfrak{F}_1(\omega) \\ \mathfrak{F}_2(\omega) \\ \mathfrak{F}_3(\omega) \end{bmatrix} = \begin{bmatrix} G_1^{+}(\omega) + G_2^{+}(\omega) \\ \xi G_1^{+}(\omega) + G_2^{+}(\omega) \\ G_1^{+}(\omega) + \xi G_2^{+}(\omega) \end{bmatrix} \tag{8}$$

The corresponding HOSIDFs follow from Lemma 1 and Definition 3 and equal:

$$H(\omega, \gamma) = \tag{9}$$
$$\begin{bmatrix} \frac{\gamma^2}{2}\mathfrak{F}_2(0) \\ \mathfrak{F}_1(\omega) + \frac{3\gamma^2}{4}\mathfrak{F}_3(\omega) \\ \frac{1}{2}\mathfrak{F}_2(2\omega) \\ \frac{1}{4}\mathfrak{F}_3(3\omega) \end{bmatrix} = \begin{bmatrix} \frac{\gamma^2}{2}\big(\xi G_1^{+}(0) + G_2^{+}(0)\big) \\ G_1^{+}(\omega) + G_2^{+}(\omega) \\ +\frac{3\gamma^2}{4}\big(G_1^{+}(\omega) + \xi G_2^{+}(\omega)\big) \\ \frac{1}{2}\big(\xi G_1^{+}(2\omega) + G_2^{+}(2\omega)\big) \\ \frac{1}{4}\big(G_1^{+}(3\omega) + \xi G_2^{+}(3\omega)\big) \end{bmatrix}$$

In the next sections, two numerical examples are presented. The first example focusses on the analysis and interpretation of the HOSIDFs while the second example illustrates the application of the theoretical results to broadband identification of the HOSIDFs in practice.

4.1 Example 1: Spectral Analysis of a $\overline{\mathbb{PL}}$ System

Consider the system depicted in Figure 2, with $\xi = 0$ and define $G_1^{+}(\omega)$ as a bandpass filter, such that $|G_1^{+}(\omega)| = 1\ \forall\ \omega \in \varpi_1$ and 0 otherwise. Furthermore, define $G_2^{+}(\omega)$ as a bandstop filter, such that $|G_2^{+}(\omega)| = 0\ \forall\ \omega \in \varpi_2$ and 1 otherwise. Finally, define the sets $\varpi_1 = [\omega_1^{-}\ \omega_1^{+}]$, $\varpi_2 = [\omega_2^{-}\ \omega_2^{+}]$ and assume that the bandstop and bandpass filters overlap, i.e. $\varpi_1 \cap \varpi_2 \neq \emptyset$.

First, consider the relation between the second and third (f)HOSIDFs, the LTI dynamics and the polynomial nonlinearities. Equation (8) and (9) provide analytical expressions for the (f)HOSIDFs for the system depicted in Figure 2. Substituting $\xi = 0$ yields the second and third fHOSIDF $\mathfrak{F}_2(\omega)$, $\mathfrak{F}_3(\omega)$ to equal the LTI dynamics $G_2^{+}(\omega)$ and $G_1^{+}(\omega)$ respectively. The corresponding HOSIDFs $\mathfrak{H}_2(\omega)$, $\mathfrak{H}_3(\omega)$ equal the same LTI dynamics, scaled in magnitude by appropriate constant ($\frac{1}{4} = -12$ dB) and contracted in ω, following Theorem 1. This is illustrated in Figure 3 where both the LTI dynamics $G_1^{+}(\omega)$, $G_2^{+}(\omega)$ and the second and third HOSIDF are depicted. Considering the

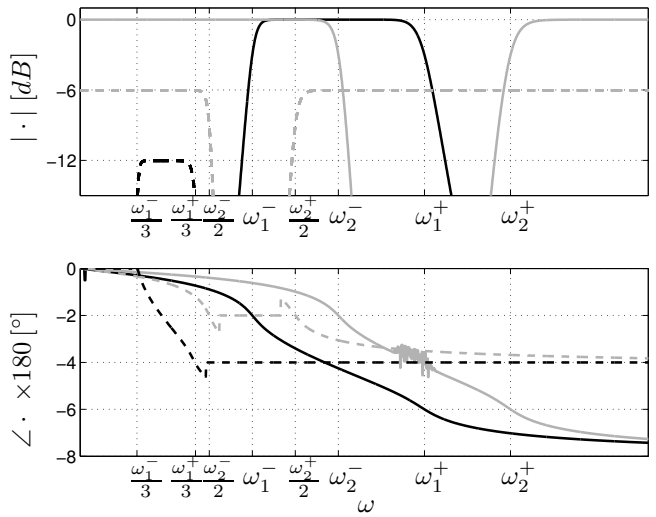

Fig. 3. LTI DYNAMICS AND HOSIDF (EXAMPLE 1): Dynamics in both branches of the system and the second and third HOSIDF.
– *(black)* $G_1^+(\omega)$, *(grey)* $G_2^+(\omega)$,
–– *(grey)* $\mathfrak{H}_2(\omega)$, *(black)* $\mathfrak{H}_3(\omega)$

third HOSIDF $\mathfrak{F}_3(\omega)$ for example, yields a bandpass filter just as $G_1^+(\omega)$. However, $\mathfrak{F}_3(\omega)$ acts on $\omega \in \frac{1}{3}\varpi_1$ and $|\mathfrak{F}_3(\omega)| = \frac{1}{4}|G_1^+(3\omega)|$.

Second, consider the effect of the nonlinearities on the first (f)HOSIDF. The first fHOSIDF is a linear combination of the LTI dynamics and is depicted in Figure 4 along with the second and third fHOSIDFs. The ripples in $|\mathfrak{F}_1(\omega)|$ originate in the numerical realization of the bandpass and bandstop filters. The fHOSIDFs are all amplitude independent by definition. Moreover, in this example the second and third HOSIDF $\mathfrak{H}_2(\omega)$, $\mathfrak{H}_3(\omega)$ are independent of the excitation level as well. However, (9) yields that $\mathfrak{H}_1(\omega)$ is amplitude dependent. This amplitude dependency is only present if $G_1^+(\omega) \neq 0$, i.e. for all $\omega \in \varpi_1$. This is illustrated in Figure 5 where the amplitude dependency is present only for $\omega \in \varpi_1$. Furthermore, note that the amplitude dependency $|\mathfrak{H}_1(\omega)| \propto \gamma^2,\ \gamma >> 1$ predicted by (9) can be observed from Figure 5 as well by an approximate 20 dB drop in magnitude over one decade change in excitation level in the appropriate frequency band.

Hence, the third order term in ρ_1 has two distinct effects on the systems dynamics, when analyzed in the frequency domain. First of all, harmonics are generated according to a scaled bandpass filter that analytically relates to the corresponding LTI dynamics. Second, an amplitude dependent response is observed at the base frequency within the frequency range on which the original bandpass filter acts. Finally, similar effects can be observed for the bandstop filter $G_2^+(\omega)$ and the related HOSIDFs $\mathfrak{H}_0(\omega)$, $\mathfrak{H}_2(\omega)$.

4.2 Example 2: Broadband Identification of HOSIDFs

In this section a numerical example is presented that illustrates the application of the theory presented in Section 3 to the identification of the HOSDIDFs of a system from broadband simulation data. Consider the system depicted in figure 2, with $\xi = \frac{1}{10}$ and the LTI dynamics $G_n^+(\omega)$ selected as different Chebyshev filters of order three. Figure 6 depicts the LTI dynamics in continuous black $G_1^+(\omega)$ and grey $G_2^+(\omega)$ lines. In the following, simulations have been performed using Matlab and all data is collected with a sampling frequency of 2560 Hz. and processed in blocks of 8192 points.

To illustrate the application of the presented theory in experimental identification techniques, the system in Figure 2 is considered as a black box model of which the structure is known but only the input $u(t)$ and output $y(t)$ can be measured. A complete discussion of the identification techniques used to obtain estimates for $G_n^+(\omega)$ and $\boldsymbol{\alpha}^{[n]}$ can be found in Schoukens et al. (2010). In short, the system is excited with a series of multisine input signal which differ in excitation level. For each level of excitation the best linear approximation of the systems dynamics is computed. Using a singular value decomposition based technique, the number of relevant branches can be selected

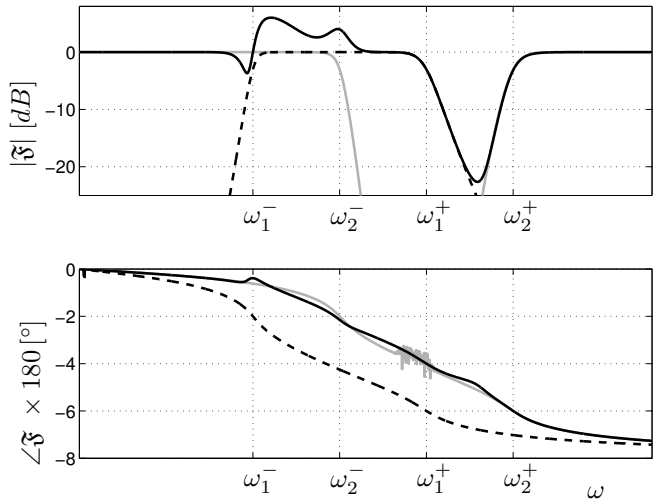

Fig. 4. fHOSIDF (EXAMPLE 1): Fundamental higher order sinusoidal input describing functions.
– (black) $\mathfrak{F}_1(\omega)$, (grey) $\mathfrak{F}_2(\omega)$, –– (black) $\mathfrak{F}_3(\omega)$

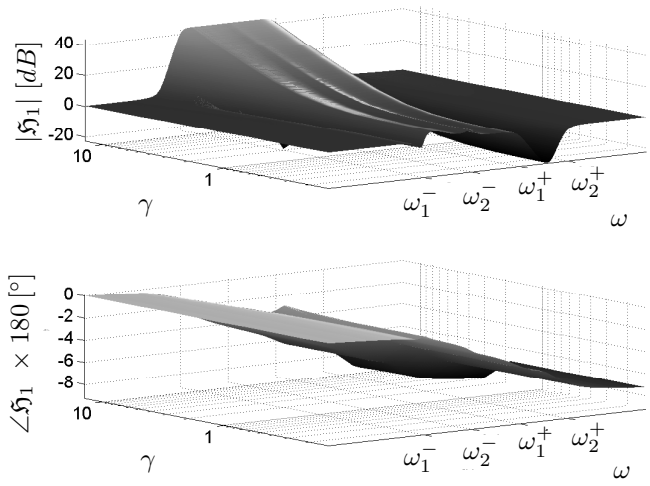

Fig. 5. FIRST HOSIDF (EXAMPLE 1): Visualization of the first HOSIDF $\hat{\mathfrak{H}}_1(\omega, \gamma)$.

and the linear dynamics $\hat{G}_n^+(\omega)$ are estimated. Finally, the parameters of the polynomial nonlinearities $\hat{\boldsymbol{\alpha}}^{[n]}$ are estimated using a least square fitting procedure on the time domain data.

During simulations, the system was excited with multisine signals with rms values ranging from 1 to 10. Therefore, the identification procedure provides a model that is valid only for this type and range of excitation. This model will generally not equal the true system dynamics and validation experiments are required to assess the quality of the estimated model. The estimated LTI models $\hat{G}_n^+(\omega)$ are depicted in Figure 6 by dashed lines and are indeed different from the true LTI dynamics $G_n^+(\omega)$. Moreover, the identified nonlinear parameters $\hat{\boldsymbol{\alpha}}^{[1]} = [1\ 0.4768\ 0.5498]^T$, $\hat{\boldsymbol{\alpha}}^{[2]} = [1\ 1.126\ \ -0.0742]^T$ differ from their true values as well. However, validation experiments within the range of excitation levels used in the experiments yield that the output predicted by the model matches the output of the true system closely. Therefore, the identified model is regarded a sufficiently accurate, local approximation of the nonlinear dynamics for the type and range of excitation used in the identification experiment.

Using the estimated LTI dynamics $\hat{G}_n^+(\omega)$ and nonlinear parameters $\hat{\boldsymbol{\alpha}}^{[n]}$, the results in Lemma 1 and Definition 3 allow to compute estimates of the fHOSIDFs $\hat{\mathfrak{F}}_p(\omega)$ and HOSIDFs $\hat{\mathfrak{H}}_k(\omega,\gamma)$, using broadband identification techniques. The advantage of this procedure is threefold. First of all, time consuming experiments are avoided where possible. Second, the HOSIDFs can be computed over a much denser grid than they can be measured in a reasonable amount of time. Finally, the HOSIDFs and possible validation experiments can be computed / measured densely in relevant or high gradient regions which are unknown a priori.

This broadband identification procedure for HOSIDFs is implemented numerically. Using a standard Matlab implementation, the first 4 HOSIDFs are computed for 2729 frequency points and 10 excitation levels, i.e. for 109160 points in 16.6 s. The first three fHOSIDFs are computed for the same number of frequency points in less than 3 ms. The total procedure, including the parametric identification of the frequency domain models and validation procedures, requires approximately 90 s.

The results of the numerical computations are shown in Figure 7 - 9. Figure 7 shows the fHOSIDFs computed by applying Definition 3 using both the identified and true LTI dynamics and the corresponding true and identified polynomial coefficients. The fHOSIDFs are amplitude independent LTI basis functions for the corresponding HOSIDFs. These HOSIDFs are computed using Lemma 1 and depicted in Figure 8. Moreover, the HOSIDFs computed using the algorithms introduced in this paper, are compared to the traditionally identified / true HOSIDFs. The difference between both is approximately -40 dB. (1%), indicating that HOSIDFs computed using broadband measurements approximate the true HOSIDFs well. Finally, Figure 9 depicts $\hat{\mathfrak{H}}_1(\omega,\gamma)$, illustrating the dependence of the HOSIDFs on both excitation amplitude and frequency.

5. CONCLUSION

The analytical results and numerical tools presented in this paper allow for novel analytical and numerically effective analysis of the output spectrum of nonlinear systems and the corresponding Higher Order Sinusoidal Input Describing Functions (HOSIDF). An analytic mapping from the parameters defining the nonlinear and LTI dynamics, to the output spectrum of a nonlinear system is provided. Using these results, the input-output behavior of class of nonlinear systems, is described using analytic expressions for the corresponding HOSIDFs. Moreover, although currently applicable to $\overline{\mathbb{LPL}}$ systems only, broadband identification techniques for HOSIDFs heavily reduce the experimental burden required to obtain the HOSIDFs.

The examples illustrate the application of the theoretical results to the frequency domain analysis of nonlinear systems. This indicates that the algorithms for broadband

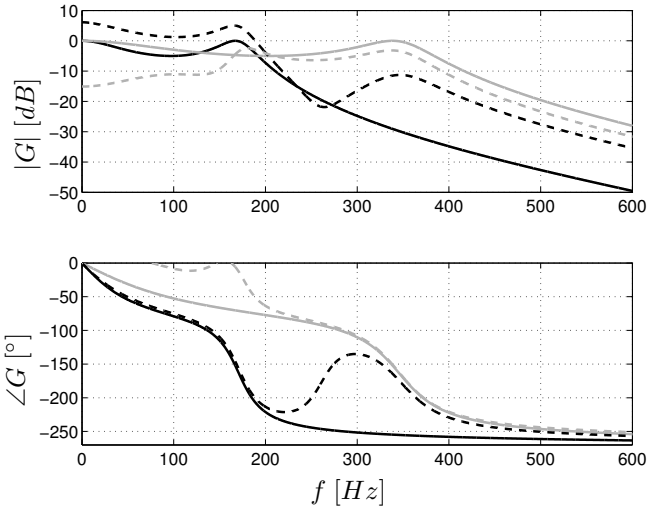

Fig. 6. LTI DYNAMICS (EXAMPLE 2): Dynamics in both branches of the true and identified system. *– True system $G_n^+(\omega)$, –– identified dynamics $\hat{G}_n^+(\omega)$. (black) First branch, (grey) second branch.*

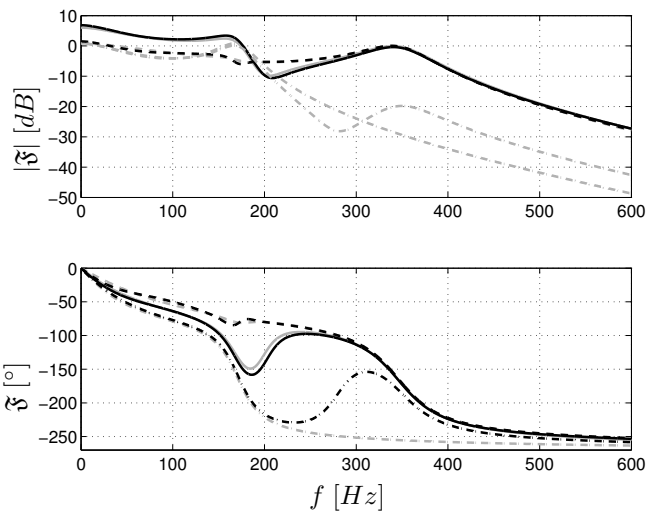

Fig. 7. fHOSIDF. Fundamental higher order sinusoidal input describing functions computed using the identified $\overline{\mathbb{PL}}$ system ⟨black⟩ and the true dynamics ⟨grey⟩. ⟨–⟩ $\mathfrak{F}_1(\omega)$, ⟨––⟩ $\mathfrak{F}_2(\omega)$, ⟨–·⟩ $\mathfrak{F}_3(\omega)$.

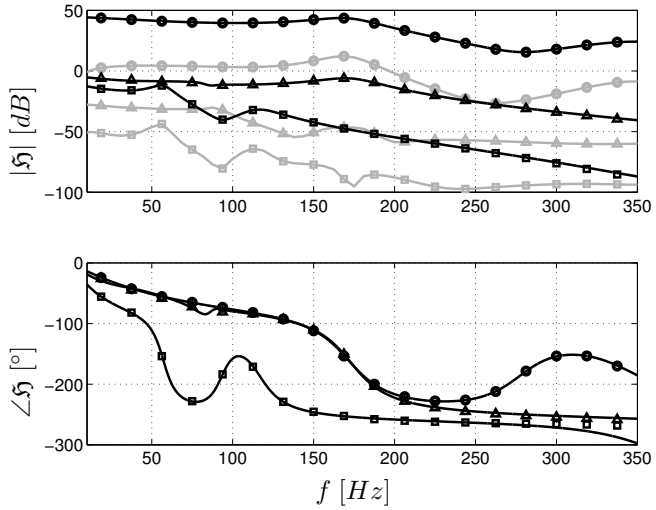

Fig. 8. HOSIDF (Example 2): Higher order sinusoidal input describing functions identified using traditional techniques based on one-tone excitation signals and using broadband identification techniques for $\gamma = 14.14$.
– (black) $\hat{\mathfrak{H}}_i(\omega,\gamma)$: HOSIDFs identified using broadband identification techniques.
$\circ$, $\triangle$, $\square$ (black) $\mathfrak{H}_i(\omega,\gamma)$: HOSIDFs of the true system, identified using one-tone excitation signals. ($\circ$ $\mathfrak{H}_1$, $\triangle$ $\mathfrak{H}_2$, $\square$ $\mathfrak{H}_3$).
$-\circ$, $-\triangle$, $-\square$ (grey) $|\mathfrak{H}_i - \hat{\mathfrak{H}}_i|$: Difference between broadband and one-tone identification techniques.

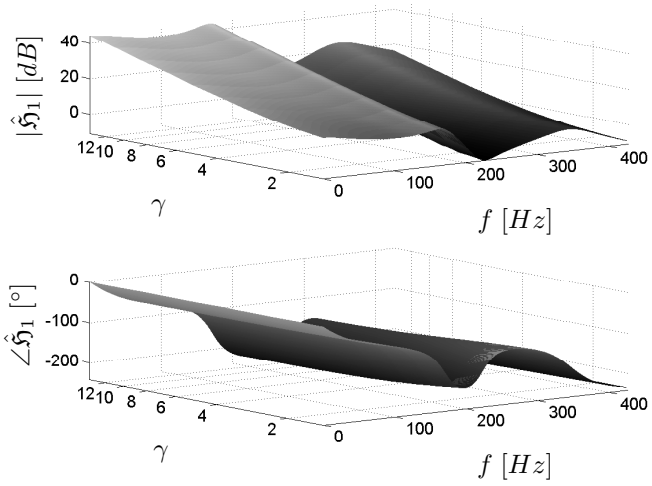

Fig. 9. First HOSIDF (Example 2): Visualization of the first HOSIDF $\hat{\mathfrak{H}}_1(\omega,\gamma)$.

identification of the HOSIDFs are applicable to experimental data as well, which is subject to current research as is further analysis of the HOSIDFs. Finally, the application of HOSIDFs to nonlinear controller design is promising and future research will focus on design and synthesis methods for nonlinear systems based on HOSIDFs.

ACKNOWLEDGEMENTS

The authors thank Maarten Schoukens for his contribution to the identification of the system presented Section 4.2.

REFERENCES

Billings, S. and Tsang, K. (1989). Spectral analysis for non-linear systems, part i: Parametric non-linear spectral analysis. *Mech Syst Signal Process*, 3(4), 319–339.

Jing, X., Lang, Z., and Billings, S. (2009). Parametric characteristic analysis for generalized frequency response functions of nonlinear systems. *Circ Syst Signal Process*, 28(5), 699–733.

Li, L. and Billings, S. (2010). Estimation of generalized frequency fresponse functions for quadratically and cubically nonlinear systems. *J Sound Vibration*. doi: 10.1016/j.jsv.2010.08.018.

Nuij, P., Steinbuch, M., and Bosgra, O. (2008a). Measuring the higher order sinusoidal input describing functions of a non-linear plant operating in feedback. *Control Eng Practice*, 16(1), 101–113.

Nuij, P., Bosgra, O., and Steinbuch, M. (2006). Higher-order sinusoidal input describing functions for the analysis of non-linear systems with harmonic responses. *Mech Syst Signal Process*, 20(8), 1883–1904.

Nuij, P., Steinbuch, M., and Bosgra, O. (2008b). Experimental characterization of the stick/sliding transition in a precision mechanical system using the third order sinusoidal input describing function. *Mechatronics*, 18(2), 100–110.

Pavlov, A., Pogromsky, A., Van De Wouw, N., and Nijmeijer, H. (2004). Convergent dynamics, a tribute to boris pavlovich demidovich. *Syst Control Lett*, 52(3-4), 257–261.

Pavlov, A., van de Wouw, N., and Nijmeijer, H. (2007a). Frequency response functions for nonlinear convergent systems. *IEEE Trans Autom Control*, 52(6), 1159–1165.

Pavlov, A., Van De Wouw, N., Pogromsky, A., Heertjes, M., and Nijmeijer, H. (2007b). Frequency domain performance analysis of nonlinearly controlled motion systems. In *Proc. CDC*, 1621–1627.

Pintelon, R. and Schoukens, J. (2001). *System identification: a frequency domain approach*. IEEE Press, NJ.

Rijlaarsdam, D., Nuij, P., Schoukens, J., and Steinbuch, M. (2010a). Frequency domain based nonlinear feed forward control design for friction compensation. *Submitted to Mech Syst Signal Process (Nov. 2010)*. Copy: david@davidrijlaarsdam.nl.

Rijlaarsdam, D., Nuij, P., Schoukens, J., and Steinbuch, M. (2010b). Spectral analysis of block structured nonlinear systems and higher order sinusoidal input describing functions. *Submitted to Automatica (Sept. 2010)*. Copy: david@davidrijlaarsdam.nl.

Rijlaarsdam, D., van Geffen, V., Nuij, P., Schoukens, J., and Steinbuch, M. (2010c). Frequency domain based feed forward tuning for friction compensation. In *Proc. ASPE spring TM*, 129–134.

Rijlaarsdam, D., van Loon, S., Nuij, P., , and Steinbuch, M. (2010d). Nonlinearities in industrial motion stages - detection and classification. In *Proc. ACC*, 6644–6649.

Schoukens, J., Lataire, J., Pintelon, R., Vandersteen, G., and Dobrowiecki, T. (2009). Robustness issues of the best linear approximation of a nonlinear system. *IEEE Trans Instr Measur*, 58(5), 1737–1745.

Schoukens, M., Pintelon, R., and Rolain, Y. (2010). Parametric identification of parallel hammerstein systems. *Submitted to IEEE Trans Instr Meas (Dec. 2010)*. Copy: maarten.schoukens@vub.ac.be.